

Electronic Supplementary Information

**Acyldhydrazone functionalized benzimidazole-based
metallogel for efficient detection and separation of Cr³⁺**

Hong Yao ^{a*}, Jiao Wang, Qi Zhou, Xiao-Wen Guan, Yan-Qing Fan, You-Ming Zhang,

Tai-Bao Wei ^{a*} and Qi Lin ^{a*}

*Key Laboratory of Eco-Environment-Related Polymer Materials, Ministry of Education of
China; Key Laboratory of Polymer Materials of Gansu Province; College of Chemistry and
Chemical Engineering, Northwest Normal University, Lanzhou, Gansu, 730070. P. R. China*

Table of contents

| | |
|--|---------------------|
| 1. ^{13}C NMR spectrum of BM . (150 MHz, 298 K) in $\text{DMSO-}d_6$. | Fig. S1. |
| 2. ^1H NMR spectrum of BM . (600 MHz, 298 K) in CDCl_3 . | Fig. S2. |
| 3. Mass spectrum of BM . | Fig. S3. |
| 4. Powder X-ray diffraction patterns of xerogel BMG , BMG-Fe and BMG-FeCr . | Fig. S4 |
| 5. Gelation property of organogelator BM . | Table S1. |
| 6. Fluorescent titrations spectra ($\lambda_{\text{ex}} = 425 \text{ nm}$) of BM ($2 \times 10^{-4} \text{ M}$) in the presence of different concentrations of (a) Fe^{3+} ; (b) Cr^{3+} ; (c) Fe^{3+} and Cr^{3+} in DMSO solution; (d) The fluorescent titrations ($\lambda_{\text{ex}} = 420 \text{ nm}$) of BMG (0.5 %, in glycerol) for Cr^{3+} (The concentration of various cations is 0.1 M, in water). | Fig. S5 |
| 8. The fluorescent spectra ($\lambda_{\text{ex}} = 420 \text{ nm}$) of metallo gel BMG-Fe (BM : $\text{Fe}^{3+} = 1: 1$, 0.5 %, in glycerol) in the presence of Al^{3+} (0.1 M, in water). | Fig. S6 |
| 7. The photograph of the fluorescent spectra linear range of (a) BMG-Fe (BM : $\text{Fe}^{3+} = 1: 1$, 0.5 %) for Cr^{3+} ; (b) BM for Fe^{3+} ; (c) BM for Cr^{3+} ; (d) BMG (0.5 %) for Cr^{3+} (The concentration of various cations is 0.1 M, in water). | Fig. S7 |
| 8. Detection limits of host gel/sol treated by metal ions. | Table S2 (a) |
| 9. Calculation formula and related date of the detection limits of BMG-Fe , BM and BMG . | Table S2 (b) |
| 10. The photograph of the linear range for BM ($2 \times 10^{-4} \text{ M}$) upon addition of different amounts of (a) Fe^{3+} and (b) Cr^{3+} ($\lambda_{\text{ex}} = 425 \text{ nm}$). | Fig. S8 |
| 11. Association constants of the BM treated by metal ions, calculation formula and related date. | Table S3 |
| 12. The titration curves of BM ($2 \times 10^{-4} \text{ M}$) with the concentration range of (a) Fe^{3+} and (b) Cr^{3+} . | Fig. S9 |
| 13. Stern–Volmer constants of the BM treated by metal ions, calculation formula and related date. | Table S4 |
| 14. Photographs of BM + Fe^{3+} ($2 \times 10^{-4} \text{ M}$) and the response of Cr^{3+} on the silica gel plate under irradiation at 365 nm by a UV lamp. | Fig. S10 |
| 15. Adsorption percentage of BMG and BMG-Fe for Cr^{3+} . | Table S5 |

| | |
|---|---------------------|
| 16. A part of the literatures about the detection limits of Cr ³⁺ were provided in the followed table. | Table S6 |
|---|---------------------|

1. Materials and physical methods

All other reagents and solvents were commercially available at analytical grade and were used without further purification. All metal ions were purchased from Alfa Aesar Chemical Reagent Co (Tianjin, China). All other reagents and solvents were commercially available at analytical grade and were used without further purification. Melting points were measured on an X-4 digital melting-point apparatus (uncorrected). ¹H NMR spectrum were recorded on a Mercury-400 BB spectrometer at 400 MHz and ¹³C NMR spectrum were recorded on a Mercury-600 BB spectrometer at 151 MHz. ¹H chemical shifts are reported in ppm downfield from tetramethylsilane (TMS, TM scale with the solvent resonances as internal standards). Mass spectra were performed on a Bruker Esquire 3000 plus mass spectrometer (Bruker-FranzenAnalytik GmbH Bremen, Germany) equipped with ESI interface and ion trap analyzer. The morphologies and sizes of the xerogels were characterized using field emission scanning electron microscopy (FE-SEM, JSM-6701F) at an accelerating voltage of 8 kV. The X-ray diffraction analysis (XRD) was performed in a transmission mode with a Rigaku RINT2000 diffractometer equipped with graphite monochromated CuK α radiation ($\lambda = 1.54073 \text{ \AA}$). The infrared spectra were performed on a Digilab FTS-3000 Fourier transform-infrared spectrophotometer. Fluorescence spectra were recorded on a Shimadzu RF-5301PC spectrofluorophotometer.

2. Synthesis and characterization of gelator **BM**

1-*N*-methoxycarbonylmethyl-2-undecyl-1*H*-benzo[d]imidazole ^{S1} (1.49 g, 4.0 mmol) was mixed in 25 mL EtOH, hydrazine (2.17 g, 40 mmol) was mixed in 25 mL EtOH, stirred at room temperature for 30 min, and then the latter slowly dripped into the former. The solution was stirred under reflux for 10 h at 80 °C. After cooling to room temperature, the solid product that appeared in the flask was filtered and recrystallized with ethanol to get crystalline product **B11** (yield: 73.6 %; m. p. 98-102 °C). Then the compound (**B11**) (1.36 g, 4 mmol) was added into a solution of 2-hydroxy naphthalene formaldehyde (0.68 g, 4 mmol) in EtOH (30 mL), the mixture was heated at 80 °C for 8 h at acetic acid (2-3 drops). After reaction was finished, the mixture was cooled to room temperature to extract the yellow-green solid. The precipitate was collected by filtration, recrystallized with DMF and EtOH and then dried in vacuum; giving a yellow-green powder compound (*E*)-*N'*-(2-hydroxynaphthalen-1-yl) methylene) -2-(2-undecyl -1*H*- benzo[d]imidazole-1-yl) acylhydrazone **BM** (1.54 g). **BM**: yield: 78.2 %; m. p. >156-160 °C; ¹³C NMR (DMSO-*d*₆, 150 MHz), δ/ppm: 167.78, 157.67, 147.26, 144.26, 133.95, 131.97, 129.3, 128.2, 123.95, 118.58, 110.61, 40.39, 31.79, 29.18, 27.23, 22.51, 14.38. Anal. Calcd. For C₃₁H₃₈N₄O₂: C, 74.67; H, 7.68; N, 11.24; O, 6.42. ¹H NMR (400 MHz, CDCl₃): δ 13.2 (d, J = 8.0 Hz, 1H, O-H), δ 12.3 (s, 1H, N-H), δ 8.17 (d, J = 5.6 Hz, 1H, N=CH), 7.9 (d, J = 6.0 Hz, 1H) 7.62-7.89 (m, 1H, ArH). ESI-MS calcd for [C₃₁H₃₈N₂O₂ + H]⁺ = 499.30; found: 499.33.

3. General procedure for ^1H NMR experiments

A series of different concentrations **BM** was respectively added into $\text{DMSO-}d_6$. The concentrations dependent ^1H -NMR of **BM** was analyzed. For the ^1H -NMR titration, the solution of **BM** and the appropriate concentrated solution of guest ions were prepared in $\text{DMSO-}d_6$. Aliquots of the two solutions were mixed directly in NMR tubes.

4. General procedure for fluorescence spectra experiments

All the fluorescence spectroscopy was carried out in DMSO solution on a Shimadzu RF-5301 spectrometer. With different equivalents perchlorate salt of cations (Ba^{2+} , Tb^{3+} , Cd^{2+} , Ag^+ , Co^{2+} , La^{3+} , Mg^{2+} , Cr^{3+} , Hg^{2+} , Ca^{2+} , Cu^{2+} , Eu^{3+} , Al^{3+} , Ni^{2+} , Zn^{2+} , Fe^{3+} and Pb^{2+}) were added into **BM** while keeping the host concentration constant (2.0×10^{-4} M) in all the experiments. The detection limits for guest ions were determined by fluorescent titrations and calculated on the basis of $3\sigma/s$ method. The addition and diffusion of appropriate equiv. of Cr^{3+} and Fe^{3+} to the **BMG** (0.5 %, in glycerol) generated the corresponding supramolecular metallogel **BMG-Fe**. Fluorescence properties of above supramolecular gels were tested at 420 nm.

5. Study of FT-IR spectroscopy

IR spectra were recorded on a Digilab FTS-3000 Fourier transform-infrared spectrophotometer. The xerogels of **BMG**, **BMG-Fe** and **BMG-FeCr** were prepared by drying a resulting gel on a glass slice for a long time. All the samples were mixed well-distributedly with KBr to create a compact pellet for the IR detection.

6. Study of scanning electron microscopy (SEM)

Determination of the SEM images was performed on a JSM-6701F FE-SEM microscope. A SEM sample was fabricated by spreading the resultant gel on a petri dish, and slow evaporated the solvent in a vacuum oven for one month. Then gold powder was sprayed on the sample after the detection system was vacuumized. The SEM image of the xerogel was determined with an accelerating voltage of 8 kV.

7. Study of X-ray diffraction analysis (XRD)

The XRD spectra of xerogels, which were fabricated by drying the resultant gels under vacuum, was performed on a Rigaku RINT2000 diffractometer equipped with graphite monochromated CuK α radiation (Cu K α radiation, $\lambda = 1.54073 \text{ \AA}$). The obtained data were collected with 2θ ranging from 0 to 60° and treated by Origin 8.5 via curve smoothing processes. The d spacing values were calculated by Bragg's law ($n\lambda = 2d \sin\theta$, d is the distance between atomic layers in a crystal or a molecular aggregate; λ is the wavelength of the incident X-ray beam; n is an integer which is generally adopted as 1)

8. General procedure for MS spectra experiments

The operation of MS spectra was carefully described according to your advice. Firstly, the organogel **BMG** (0.5 %, in glycerol) was prepared in glycerol, and then adding 1.0 equiv. Fe $^{3+}$ followed by 1.0 equiv. Cr $^{3+}$ into **BMG** (according to the detection limit of **BMG** for Fe $^{3+}$ and Cr $^{3+}$) formed metallogel **BMG-FeCr**. Thirdly, a xerogel sample was fabricated by spreading the resultant metallogel on a petri dish, and slow evaporated the solvent in a vacuum oven for a period of time. The MS spectra were operated by laboratory manager.

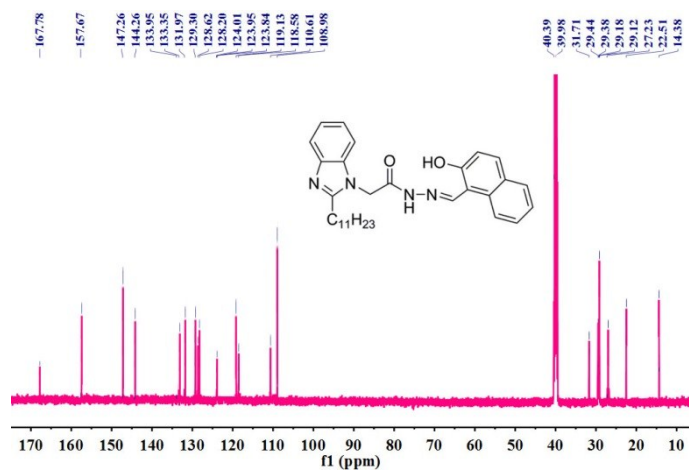


Fig. S1. ^{13}C NMR spectrum (150 MHz, 298 K) of **BM** in $\text{DMSO-}d_6$.

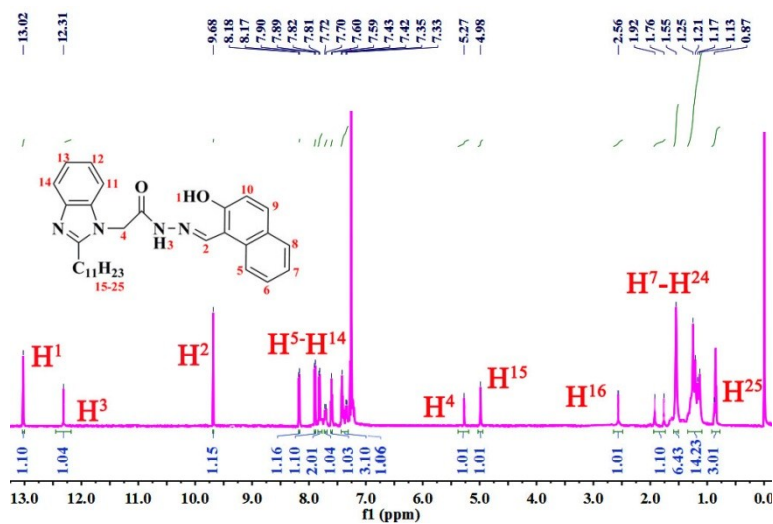


Fig. S2. ^1H NMR spectrum (600 MHz, 298 K) of **BM** in CDCl_3 .

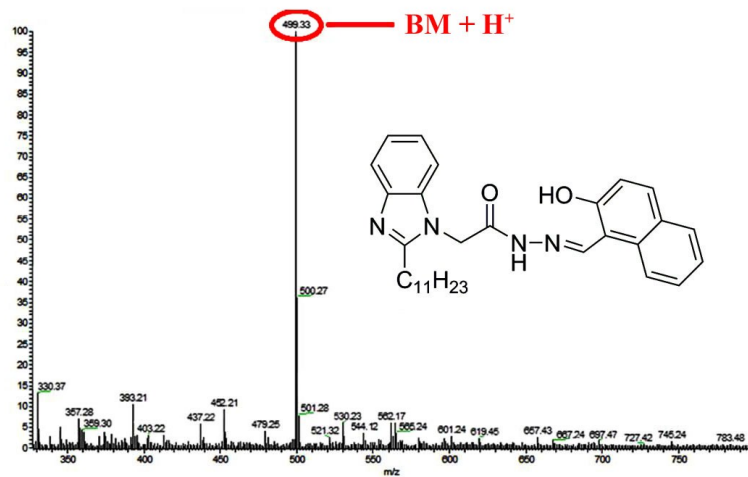


Fig. S3. Mass spectrum of BM.

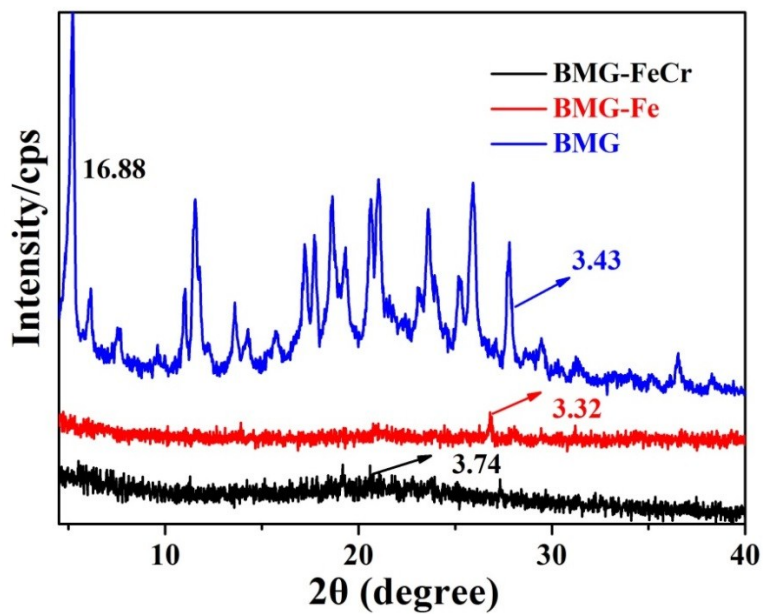


Fig. S4. Powder X-ray diffraction patterns of xerogel BMG, BMG-Fe and BMG - FeCr.

Table S1. Gelation Property of organogelator **BM**.

| Solvent | Gelation behavior ^a | ^b T _{gel} (°C, wt %) | CGC (%) |
|----------------------|--------------------------------|--|-------------|
| MeOH | P | — | — |
| EtOH | P | — | — |
| n-PrOH | P | — | — |
| i-PrOH | S | — | — |
| n-BuOH | S | — | — |
| t-BuOH | SP | — | — |
| i-PeOH | S | — | — |
| Cyclohexanol | S | — | — |
| Acetone | S | — | — |
| Ethylene glycol | G | 23°C (1 %) | — |
| Acetonitrile | P | — | — |
| Ethyl acetate | P | — | — |
| DMSO | S | — | — |
| Tert-butanol | S | — | — |
| DMF | S | — | — |
| Glycerol | G | 43°C (1 %) | 0.5% |
| Dichloromethane | S | — | — |
| Chloroform | S | — | — |
| Carbon tetrachloride | P | — | — |

^a G, gel ; S, solution ; SP, solution precipitate (wt %, w/v, 10 mg mL⁻¹ = 1.0 %)

^b T_{gel}: The gel-sol transition temperature (°C)

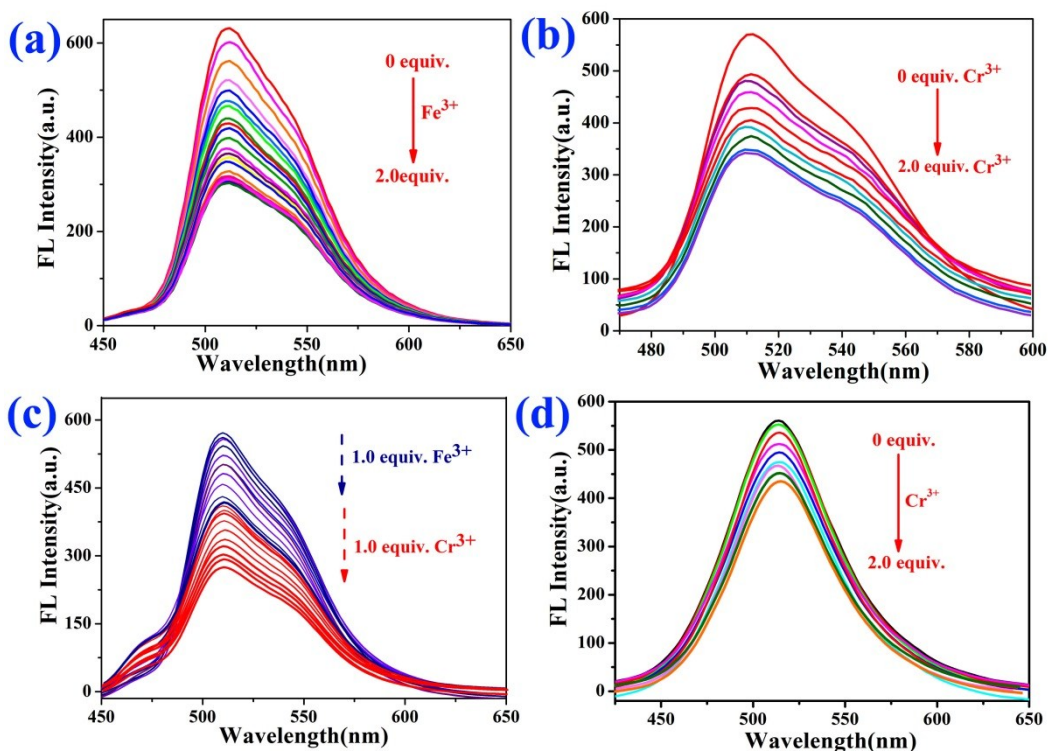


Fig. S5 Fluorescent titrations spectra ($\lambda_{\text{ex}} = 425 \text{ nm}$) of **BM** ($2 \times 10^{-4} \text{ M}$) in the presence of different concentrations of (a) Fe^{3+} ; (b) Cr^{3+} ; (c) Fe^{3+} and Cr^{3+} in DMSO solution; (d) The fluorescent titrations ($\lambda_{\text{ex}} = 420 \text{ nm}$) of **BMG** (0.5 %, in glycerol) for Cr^{3+} (The concentration of various cations is 0.1 M, in water).

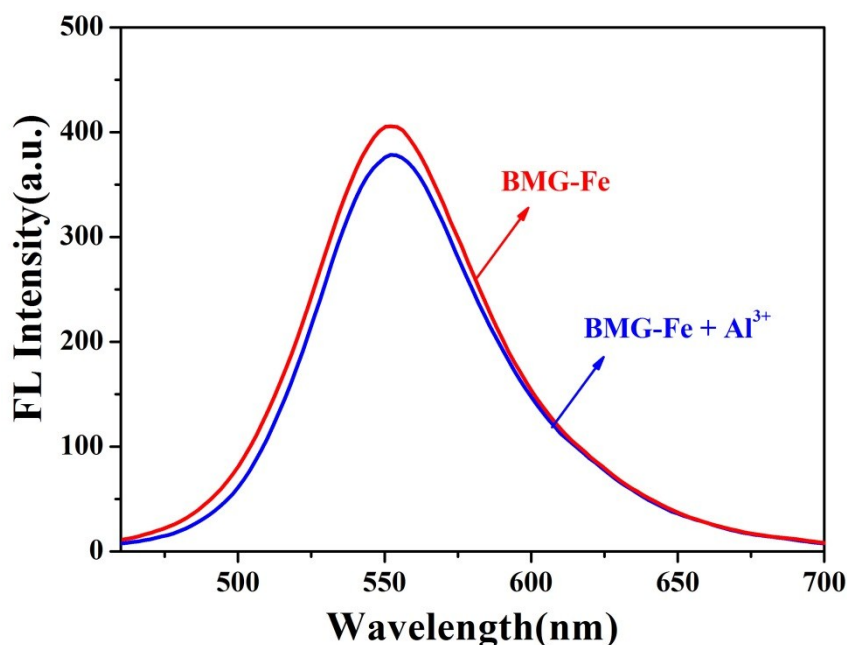
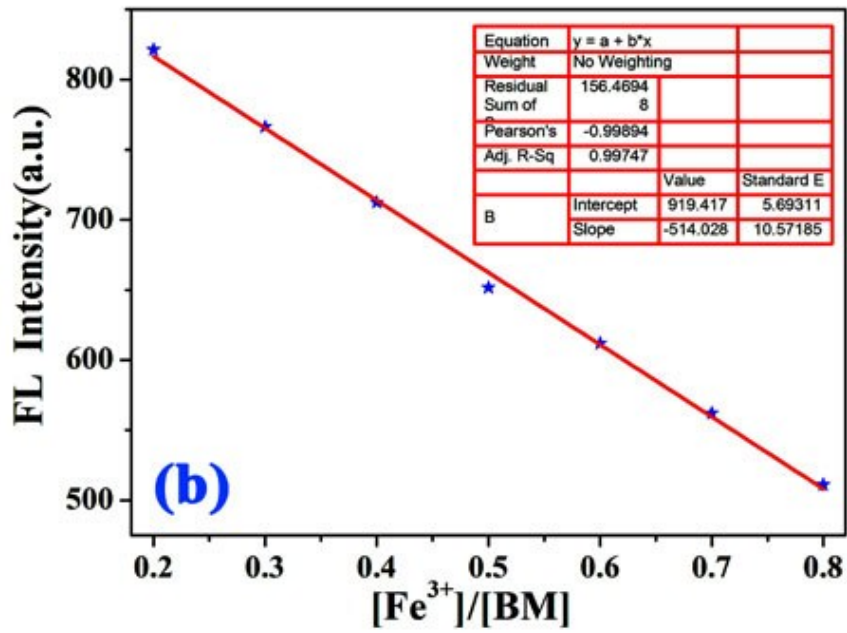
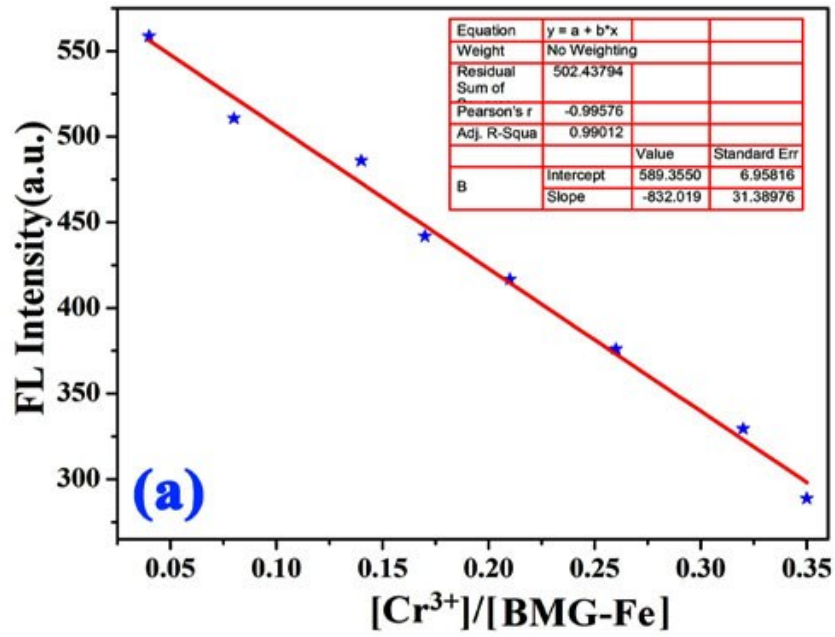


Fig. S6. The fluorescent spectra ($\lambda_{\text{ex}} = 420 \text{ nm}$) of metallogel **BMG-Fe** (**BM**: $\text{Fe}^{3+} = 1:1$, 0.5 %, in glycerol) in the presence of Al^{3+} (0.1 M, in water).



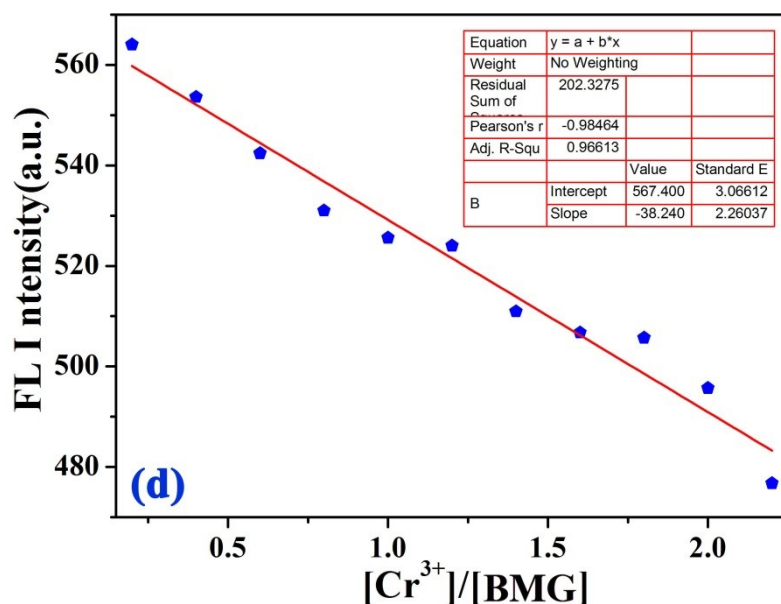
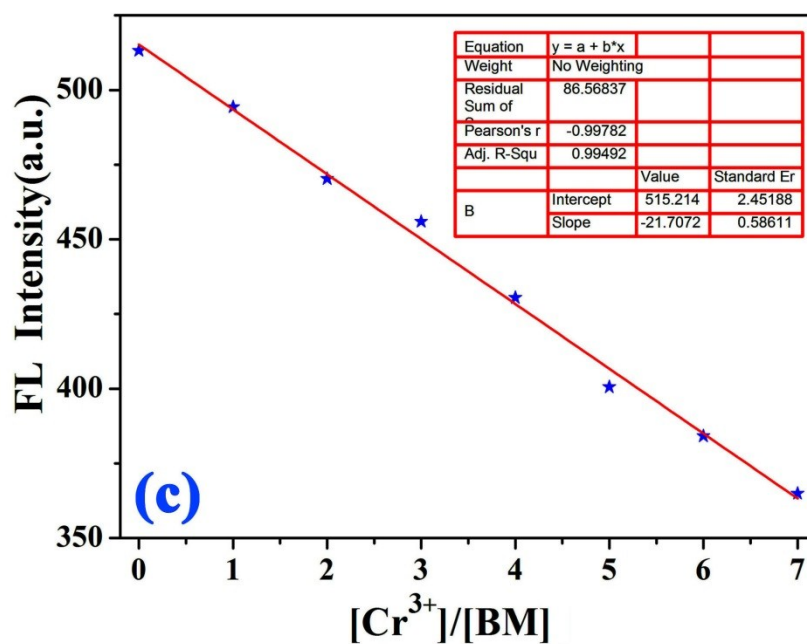


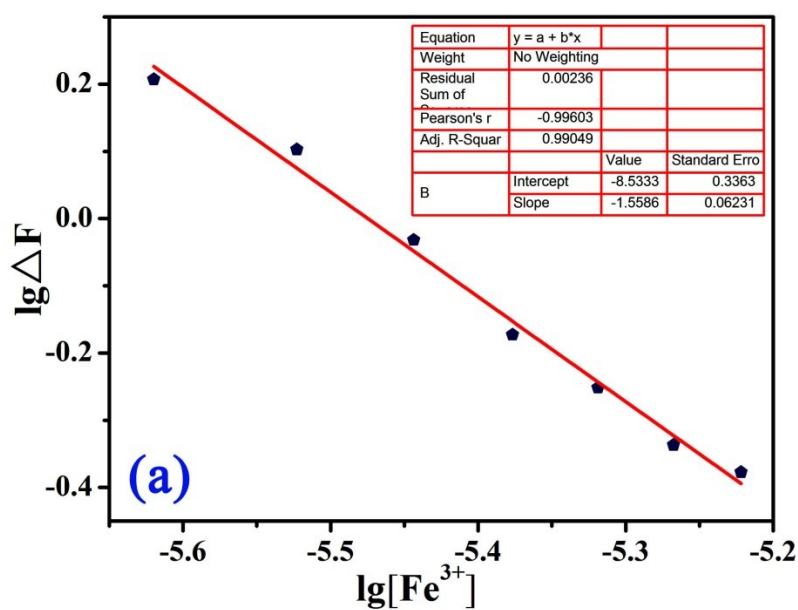
Fig. S7 The photograph of the fluorescent spectra linear range of (a) **BMG-Fe** (**BM**: $\text{Fe}^{3+} = 1: 1, 0.5 \%$) for Cr^{3+} ; (b) **BM** for Fe^{3+} ; (c) **BM** for Cr^{3+} ; (d) **BMG** (0.5 %) for Cr^{3+} (The concentration of various cations is 0.1 M, in water).

Table S2 (a) Detection limits of host gel/sol treated by metal ions.

| Entry | Gel/Sol | Metal ions | Detection limits/M |
|-------|---------|------------------|-----------------------|
| 1 | BMG-Fe | Cr^{3+} | 2.62×10^{-8} |
| 2 | BM | Cr^{3+} | 5.57×10^{-7} |
| 3 | BM | Fe^{3+} | 5.78×10^{-8} |
| 4 | BMG | Cr^{3+} | 1.89×10^{-4} |

Table S2 (b) Calculation formula and related data of the detection limits of **BMG-Fe**, **BM** and **BMG**.

| Entry | A (Slope) | B (Intercept) | R ² | S |
|---|--------------------------------------|---------------|----------------|---------------------------|
| 1 | 832.019 | 589.355 | 0.99012 | 8.32028 × 10 ⁸ |
| 2 | 21.7072 | 515.214 | 0.99492 | 1.68366 × 10 ⁶ |
| 3 | 514.028 5.14038 × 10 ⁸ | 919.417 | 0.99747 | |
| 4 | 38.2400 3.82408 × 10 ⁷ | 567.400 | 0.99613 | |
| <p>Linear Equation: y = Ax + B</p> <p>calculation formula</p> $\delta = \sqrt{\frac{\sum (F - \bar{F})^2}{(N - 1)}} \quad (N = 20) \quad K = 3$ <p>LOD = K × δ/s</p> <p>S = A × 10⁶</p> | | | | |



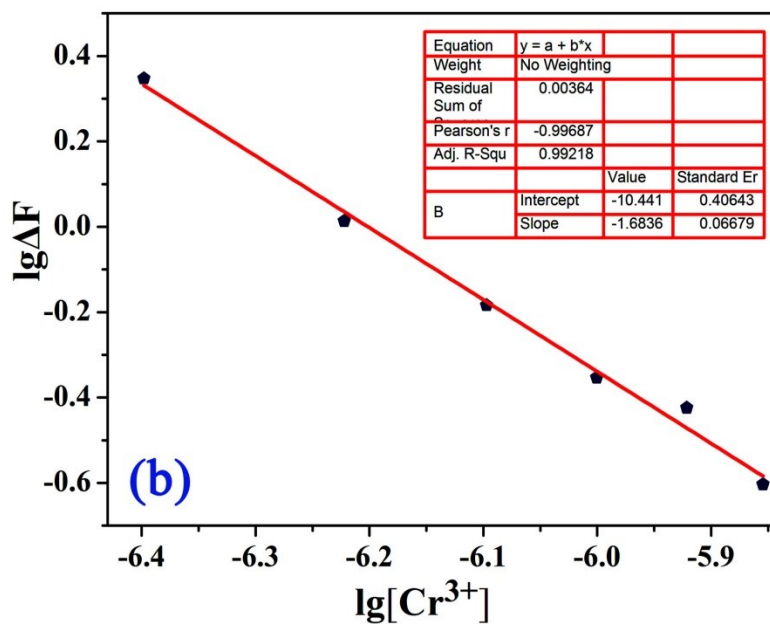


Fig. S8 The photograph of the linear range for **BM** (2×10^{-4} M) upon addition of different amounts of (a) Fe^{3+} and (b) Cr^{3+} ($\lambda_{\text{ex}} = 425$ nm).

Table S3. Association constants of the BM treated by metal ions, calculation formula and related date.

| Entry | Metal ions | A (Slope) | B (Intercept) | R ² | Ka/ M ⁻² |
|----------------------------------|--|-----------|---------------|----------------|-----------------------|
| 1 | Fe^3 | 1.5586 | 8.5333 | 0.99049 | 7.87×10^{11} |
| 2 | Cr^{3+} | 1.6836 | 10.441 | 0.99218 | 2.96×10^9 |
| Linear Equation: y=Ax + B | | | | | |
| calculation formula | $\log \frac{I - I_{\text{min}}}{I_{\text{max}} - I} = \log Ka + n \log [M^{3+}]$ | | | | |

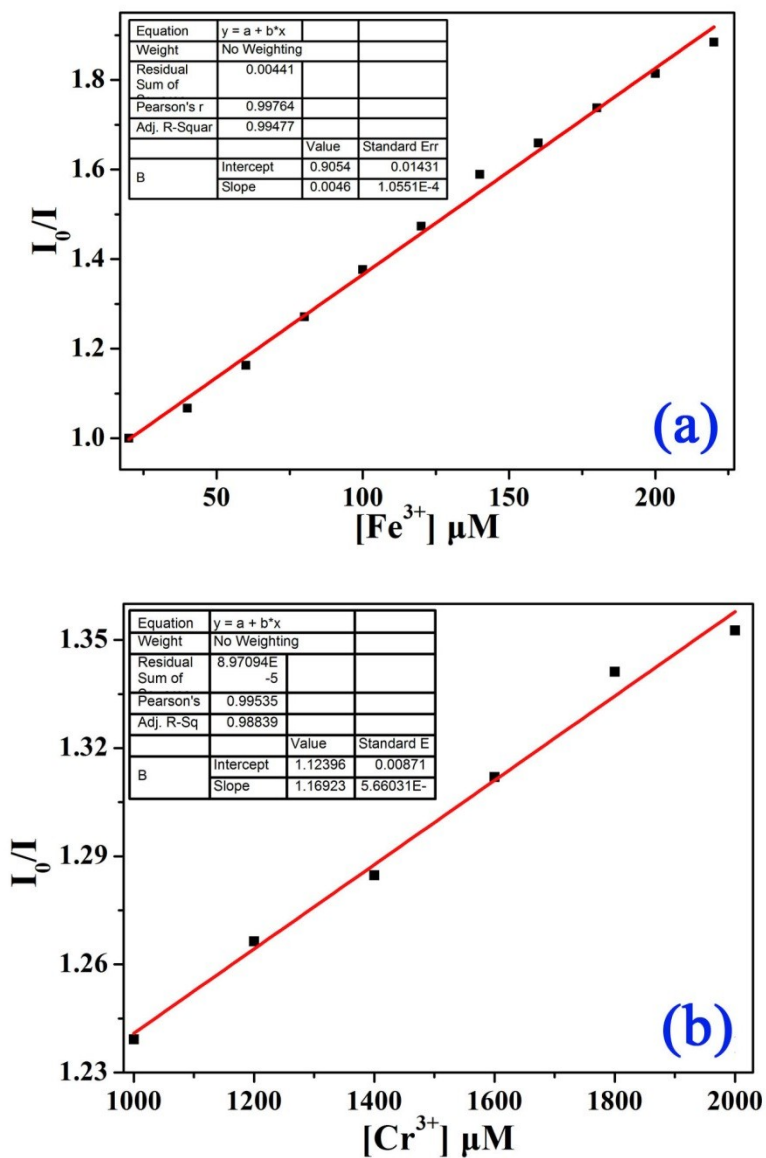


Fig. S9 The titration curves of **BM** (2×10^{-4} M, in DMSO) with the concentration range of (a) Fe^{3+} and (b) Cr^{3+} .

Table S4. Stern–Volmer constants of the **BM** treated by metal ions, calculation formula and related date.

| Entry | Metal ions | A (Slope) | B (Intercept) | R ² | K _{sv} / M ⁻¹ |
|---------------------|--|-----------|---------------|----------------|-----------------------------------|
| 1 | Fe ³ | 0.0046 | 0.9054 | 0.99477 | 4.60×10^3 |
| 2 | Cr ³⁺ | 1.6923 | 1.1240 | 0.98839 | 1.16×10^6 |
| calculation formula | Linear Equation: $y = Ax + B$ $I_0/I = 1 + K_{SV}[Q]$ | | | | |

The Stern–Volmer quenching equation:

$$I_0/I = 1 + K_{SV} [Q]$$

Where, I_0 represents the initial fluorescence intensity of **BM** prior to the addition of analyte;

I represents fluorescence intensity after addition of analyte;

$[Q]$ represents the molar concentration of analytes, and K_{SV} represents the Stern–Volmer constant.

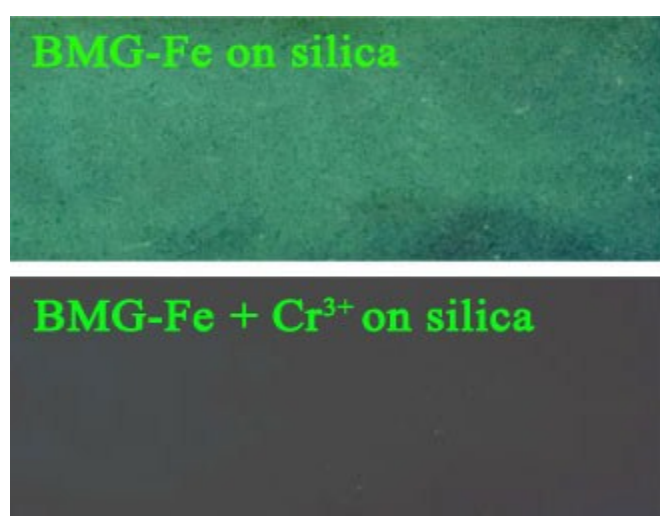


Fig. S10 Photographs of **BMG-Fe** (2×10^{-4} M) and the response of Cr^{3+} on the silica gel plate under irradiation at 365 nm by a UV lamp.

Table S5 Adsorption percentage of **BMG** and **BMG-Fe** for Cr^{3+} .

| substance | Ions | Initial concentration (M) | Residual concentration (M) | Adsorption percentage % |
|---------------|------------------|---------------------------|----------------------------|-------------------------|
| BMG-Fe | Cr^{3+} | 1×10^{-4} | 3.64×10^{-6} | 96.36% |
| BMG | Cr^{3+} | 1×10^{-4} | 1.64×10^{-5} | 83.60% |

Calculation method of adsorption percentage:

$$\text{Adsorption percentage}(\%) = \left(1 - \frac{C_R \times V_R}{C_I \times V_I}\right) \times 100\%$$
 (state: C_R is the residual concentration of Cr^{3+} , C_I is the initial concentration of Cr^{3+} , $V_R=V_I$)

Table S6 A part of the literatures about the uptake of Cr^{3+} were provided in the followed table.

| Author | Journal and Year. Volume. Page | Adsorption percentage for Cr ³⁺ |
|----------------------------|--|--|
| Kai-Feng Du. etc | Ind. Eng. Chem. Res. 2013, 52, 6502-6512 | 95.61% |
| Kai-Feng Du. etc | Ind. Eng. Chem. Res. 2011, 50, 10784– 10791 | 82.4% (PH=6.42) 87.6% (PH=5.03) |
| Qi Lin etc | Chem. Eur. J. 2017, 23, 1–8 | 95.99% |
| This work | | 96.36% |

S1 H. Yao, H. P. Wu, J. Chang, Q.Lin, T. B. Wei and Y. M. Zhang, *New J. Chem.*, 2016, **40**, 4940-4944.